Estimation of particle size distribution in multiple small-angle scattering

1995 J. Phys.: Condens. Matter 7 9737

(http://iopscience.iop.org/0953-8984/7/50/008)

J. Phys.: Condens. Matter 7 (1995) 9737–9746. Printed in the UK

Estimation of particle size distribution in multiple small-angle scattering

S Mazumder, K V Bhagwat and A Sequeira
Solid State Physics Division, Bhabha Atomic Research Centre, Bombay 400 085, India

Received 9 June 1995, in final form 5 September 1995

Abstract. The possibility of employing the maximum-entropy method to extract the particle size distribution from a multiple-small-angle-scattering profile is examined. The sensitivity of the method to the choice of different prior distribution conditions is investigated. The various maximum-entropy-estimated results are compared with three model distributions, namely the log–normal, Weibull and Gaussian distributions for particle size.

1. Introduction

The characterization of particle size distribution (PSD) is very important in small-angle-scattering (SAS) studies dealing with materials science. The use of conventional SAS in estimation of PSDs is limited to thin samples, a weak-scattering medium and particles with relatively small size.

SAS data for many materials are affected by multiple scattering more often than is normally conceived. The influence of multiple scattering in SAS data comes from one or more of factors like strong contrast, long wavelength, large inhomogeneities and significant thickness of the sample—which cannot be reduced indefinitely for practical reasons. In SAS studies, multiple scattering can even be exploited [1] to study inhomogeneities that are much larger than is permitted by the resolution constraint of the instrument for conventional SAS. Further, since multiple scattering enhances the scattering signal, it is possible to make use of a weak source for SAS study if multiple scattering is suitably exploited.

The extent of multiple scattering depends upon the thickness of the sample in relation to the scattering mean free path. It is possible to extract a single-scattering profile quite convincingly from multiple-scattering data for samples with thicknesses less than ten times the scattering mean free path. But when the thickness is larger than ten times the scattering mean free path, the particle size distribution can be estimated from the multiple-scattering data alone, avoiding the extraction of a single-scattering profile. In the present investigation, we are concerned with studies where the thickness of the sample is more than ten times the scattering mean free path.

The particle size distribution can be conveniently extracted from a multiple-small-angle-scattering (MSAS) profile under the assumption of a model distribution. For real systems commonly used, model particle size distributions include the log–normal (LN), Gaussian (G) and Weibull (WB) distributions. The usefulness of variational techniques, in particular the maximum-entropy method [2], for data inversion is now being realized. It is worth mentioning some of the recent efforts which have exploited this technique to get an estimate of either the PSD [3–7] or the pair distribution function [8, 9] from conventional

0953-8984/95/509737+10$19.50

SAS profiles. However, to our knowledge, the maximum-entropy technique has not been employed for obtaining an estimate of the PSD from MSAS profiles. The present paper is a step in that direction.

2. Theory

2.1. Scattering laws for multiple small-angle scattering

In MSAS, the scattering laws are described [10] in terms of a normalized density function $F(q)$ ($\int F(q)\,d\Omega = 1$) where q denotes the wave-vector transfer.

The angular distribution of the radiation, for a $\delta(q)$ incident beam, passing through the sample is given [10] by

$$\delta(q)\exp(-\mu_a Z - N) + (1 - e^{-N})\exp(-\mu_a Z)F(q) \tag{1}$$

where μ_a is the macroscopic absorption coefficient of the sample, N is the average number of SASs that the interaction radiation has undergone while passing through the sample, of thickness Z. For a monodisperse system of spherical particles of radius R and scattering length density D, $N = 2\pi\rho Z\lambda^2 D^2 R^4$ where ρ is the number density of the inhomogeneity of radius R in the sample, and λ is the wavelength of the radiation. In the case of a polydisperse system, with degree of polydispersity n, N is given by

$$N = 2\pi Z\lambda^2 \sum_{i=1}^{n} \rho_i D_i^2 R_i^4 \tag{2}$$

where the subscripted quantities ρ_i, D_i and R_i are respectively the number density, scattering length density and radius of the ith type of particle. The fraction of the incident radiation absorbed in the sample is given by $(1 - e^{-\mu_a Z})$.

The differential scattering cross section $S(q)$ of the sample is given by

$$S(q) = A(1 - e^{-N})F(q) \tag{3}$$

where A is the area of the sample surface exposed to the incident beam.

The differential scattering cross section $S_v(q)$ per unit volume of the sample is given by

$$S_v(q) = (1 - e^{-N})F(q)/Z. \tag{4}$$

For conventional SAS, since $N \approx 0$, $1 - e^{-N} \approx N$, whereas for MSAS $1 - e^{-N} \approx 1$ since $N \gg 1$.

Now let us consider the nature of the scattering profile for a polydisperse system. For the present discussion, we assume that the sample under study consists of a large variety of spherical scattering particles. The volume fraction of the ith type of particle in the sample is denoted by p_i while Γ_i and μ_{a_i} are respectively its differential scattering cross section and macroscopic absorption coefficient.

When the linear dimensions of the particles are negligible in comparison with the mean free path of the radiation inside the medium, it is possible [10] to define an effective single-scattering cross section $\sum_i \rho_i \Gamma_i$ and absorption coefficient $\sum_i p_i \mu_{a_i}$ for the medium. Such a polydisperse medium is termed a *effective medium.*

We will restrict our present discussion to scattering profiles for scattering from a polydisperse effective medium only. We assume that different particles have the same scattering length density contrast D.

2.1.1. The Guinier regime. The scattering profile in the Guinier regime is represented [10] by

$$\lim_{q\to 0} F_{MSAS}(q) = \frac{2\langle R^3\rangle k^2}{15\langle R^2\rangle \pi Z\tau\lambda^2 D^2}\exp\left(-\frac{2\langle R^3\rangle q^2}{15\langle R^2\rangle Z\tau\lambda^2 D^2}\right) \tag{5}$$

where τ denotes the packing fraction of the sample. The above relation indicates that the information extractable from the Guinier regime for a MSAS profile from a polydisperse system is given by

$$\langle R^3\rangle/\langle R^2\rangle = \sum_i \rho_i R_i^3 \Big/ \sum_i \rho_i R_i^2 \tag{6}$$

for a continuous distribution of particles. This fact has been verified [1] by experiment recently.

2.1.2. The Porod regime. The scattering profile in the Porod regime is given by

$$\lim_{q\to\infty} F_{MSAS}(q) = \frac{4\pi}{\lambda^2}\frac{\langle R^2\rangle}{\langle R^4\rangle}q^{-4} \tag{7}$$

indicating that the nature of the information extractable from the Porod regime for the multiple-scattering profile is given by the ratio $\langle R^4\rangle/\langle R^2\rangle$.

2.2. Particle size distribution

Now let us discuss how to obtain the particle size distribution $\rho(R)$ from the information on moment ratios, namely, $a \equiv \langle R^3\rangle/\langle R^2\rangle$ and $b \equiv \langle R^4\rangle/\langle R^2\rangle$ obtained from the MSAS profile. In the discussion to follow, we will express R in units of 1000 Å and hence it will be treated as a dimensionless quantity.

As mentioned in the introduction, one way to obtain the particle size distribution is to employ a model distribution function involving a certain number of adjustable parameters. Among the commonly used model particle size distributions, the LN distribution is the simplest for analytical calculation purposes. The required moment ratios can be computed exactly. The function $\rho_{LN}(R)$ is given by

$$\rho_{LN}(R) = \left(\frac{Y}{R\sqrt{2\pi}}\right)\exp[-(w + Y\ln R)^2/2] \tag{8}$$

where Y and w are to be obtained from the moment ratio constraints

$$\langle R^3\rangle/\langle R^2\rangle = \exp[(5/2)Y^{-2} - wY^{-1}] \tag{9}$$

and

$$\langle R^4\rangle/\langle R^2\rangle = \exp[6Y^{-2} - 2wY^{-1}]. \tag{10}$$

We shall also explicitly describe the two other models often employed for the particle size distribution. The WB distribution is given by

$$\rho_{WB}(R) = c(R/R_0)^{b-1}\exp[-(R/R_0)^b] \tag{11}$$

where c is the normalization constant and R_0 and b are adjustable parameters. The G distribution is well known and is written in the form

$$\rho_G(R) = c\exp[-(R-\alpha)^2/\beta]. \tag{12}$$

Here c is the normalization constant and α and β are the model parameters.

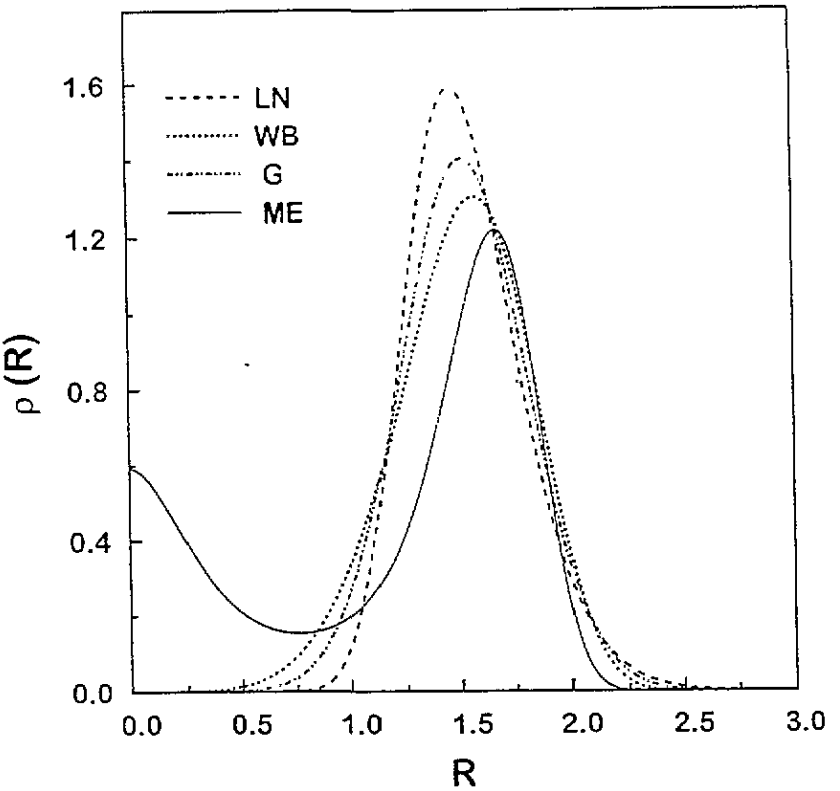

Figure 1. Estimation of the particle size distribution $\rho(R)$ from the assumed values of the moment ratios $\langle R^3\rangle/\langle R^2\rangle = 1.62$ and $\langle R^4\rangle/\langle R^2\rangle = 2.7$. Three model distributions—the log-normal, Gaussian and Weibull—are plotted along with the maximum-entropy distribution with $g(R) = 1$.

Now let us obtain the distribution which is statistically most probable—the maximum-entropy distribution. As the name suggests, it has a maximum entropy or uncertainty associated with it. This is obtained by maximizing a certain entropy functional subject to fixed moment ratios. In the present case where we assume a continuum of possible radii for the spherical particles the moment ratios are given by

$$a \equiv \frac{\langle R^3\rangle}{\langle R^2\rangle} = \int \rho(R)R^3\,\mathrm{d}R \Big/ \int \rho(R)R^2\,\mathrm{d}R \tag{13}$$

$$b \equiv \frac{\langle R^4\rangle}{\langle R^2\rangle} = \int \rho(R)R^4\,\mathrm{d}R \Big/ \int \rho(R)R^2\,\mathrm{d}R. \tag{14}$$

The Bayesian entropy functional of the distribution is given by

$$S = -\int \rho(R)\ln[\rho(R)/g(R)]\,\mathrm{d}R. \tag{15}$$

where $g(R)$ is the prior distribution—a default distribution in the absence of any constraints, that is, when we do not know the values of the moment ratios a and b.

From the normalization condition of $\rho(R)$, we have

$$\int \rho(R)\,\mathrm{d}R = 1. \tag{16}$$

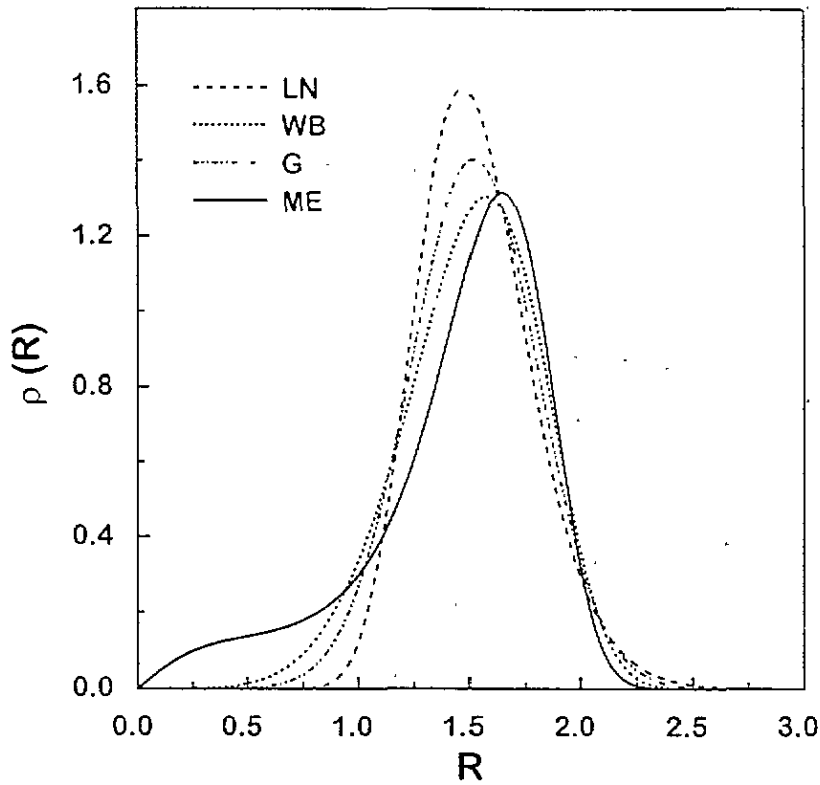

Figure 2. As figure 1, but with $g(R) = R$.

It is convenient to express the constraints by the equations

$$\int \rho(R)[R^3 - aR^2]\,\mathrm{d}R = 0 \tag{17}$$

and

$$\int \rho(R)[R^4 - bR^2]\,\mathrm{d}R = 0. \tag{18}$$

Introducing Lagrange multipliers $(\alpha - 1)$, α_1 and α_2, for each of the constraints (16) , (17) and (18), we construct the functional

$$G = -\int \rho(R) \ln\left(\frac{\rho(R)}{g(R)}\right)\,\mathrm{d}R + (\alpha - 1)\left(\int \rho(R)\,\mathrm{d}R - 1\right)$$
$$+\alpha_1 \int \rho(R)[R^3 - aR^2]\,\mathrm{d}R + \alpha_2 \int \rho(R)[R^4 - bR^2]\,\mathrm{d}R \tag{19}$$

which can be maximized subject to arbitrary variation $\delta\rho(R)$ in $\rho(R)$. Following the standard procedure we obtain

$$\rho(R) = g(R)\exp(-\alpha - \alpha_1(R^3 - aR^2) - \alpha_2(R^4 - bR^2)). \tag{20}$$

This is the maximum-entropy distribution. For a complete knowledge of $\rho(R)$ we need to know the values of the Lagrange multipliers. From equations (16) and (20), we obtain

$$\alpha = \ln\left[\int g(R)\exp(-\alpha_1(R^3 - aR^2) - \alpha_2(R^4 - bR^2))\,\mathrm{d}R\right]. \tag{21}$$

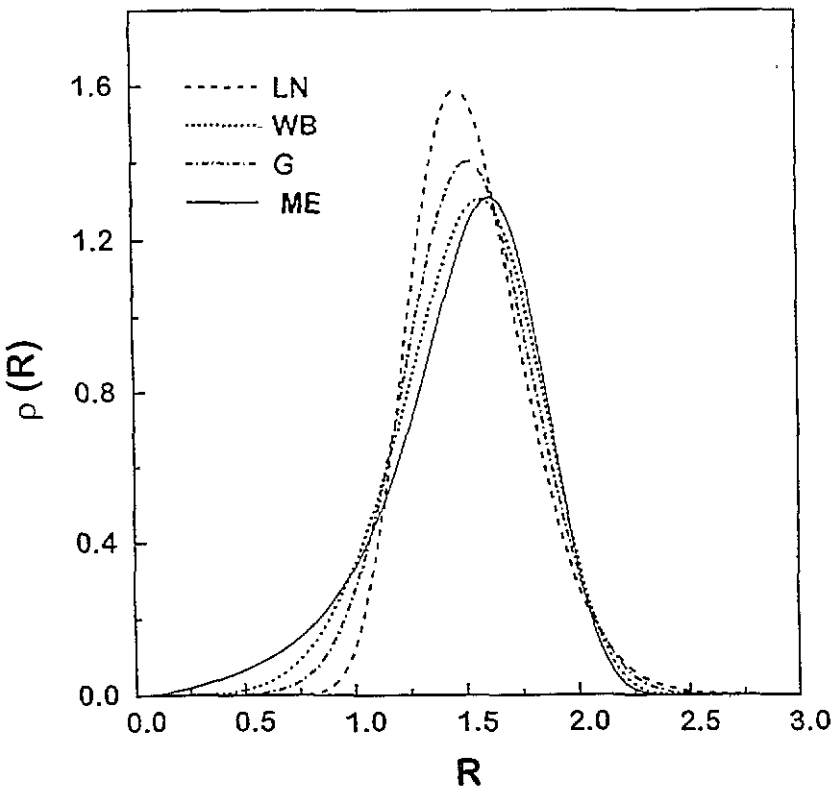

Figure 3. As figure 1, but with $g(R) = R^2$.

Equation (21) expresses α in terms of α_1 and α_2. This is expected because α arises due to the simple normalization condition on $\rho(R)$. To obtain the values of α_1 and α_2, we substitute the expression (20) for $\rho(R)$ in equations (17) and (18) and obtain two coupled equations involving α_1 and α_2:

$$\int_0^\infty (R^3 - aR^2)g(R)\exp(-\alpha_1(R^3 - aR^2) - \alpha_2(R^4 - bR^2))\,\mathrm{d}R = 0 \qquad (22)$$

$$\int_0^\infty (R^4 - bR^2)g(R)\exp(-\alpha_1(R^3 - aR^2) - \alpha_2(R^4 - bR^2))\,\mathrm{d}R = 0. \qquad (23)$$

The values of α_1 and α_2 are obtained by solving equations (22) and (23) numerically.

It is to be noted that in the expression for $\rho(R)$, α_2 has to be positive, otherwise the distribution will diverge with increasing value of R.

3. Numerical results and discussion

We now consider a special case where the moment ratios have typical values $a = 1.62$ and $b = 2.7$. These numbers are typical in the sense that they are close to actual numbers obtained from an experimental MSAS profile.

First let us consider the model distributions given in section 2. We determine the adjustable parameters so that we get the above numbers for the moment ratios. Thus we have $w = -2.4414$ and $Y = 5.933\,963$ for the LN distribution, $b = 5.676\,76$ and

$R_0 = 1.62628$ for the WB distribution and $\alpha = 1.51723$ and $\beta = 0.16139$ for the G distribution.

Along with these we also obtain the maximum-entropy estimate (MEE) for the particle size distribution. Its determination, as seen in section 2, requires knowledge of the prior distribution function. In this regard the studies carried out in the literature so far do not lead to any unique answer—for the only prior knowledge one has is that any plausible particle size distribution function should vanish at $R = 0$ and also as $R \to \infty$. A prior distribution that is uniform over some range $R_0 \leqslant R \leqslant R_c$ and vanishing outside this range is often recommended. This is presumably done to ensure that the prior distribution is a proper (normalizable) distribution function. This restriction may, however, be relaxed [2]. Thus one may use an improper prior distribution function provided the eventual maximum-entropy distribution obtained therefrom is proper.

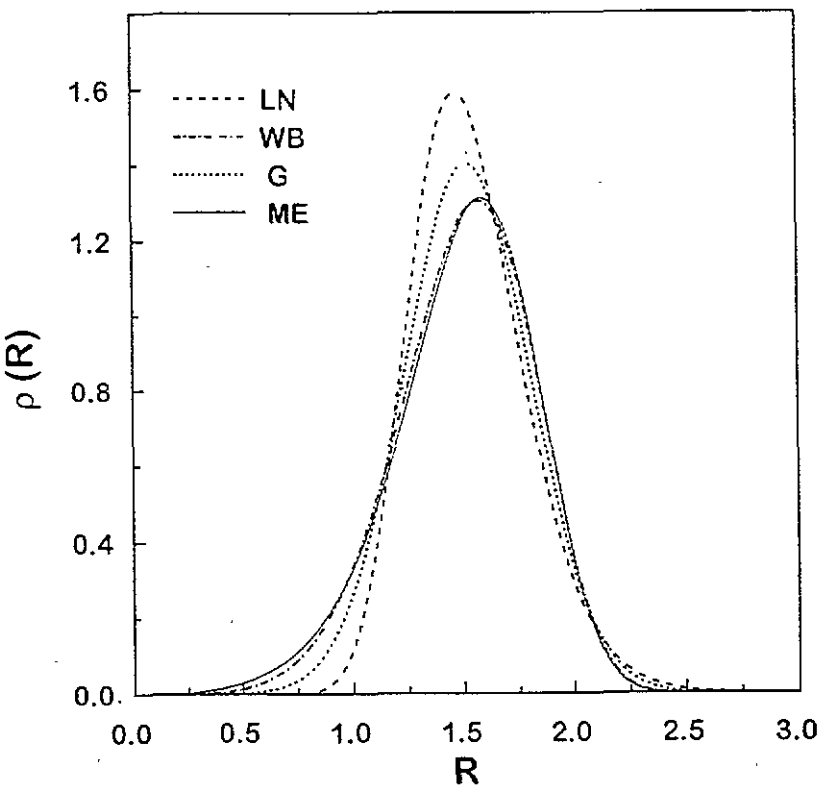

Figure 4. As figure 1, but with $g(R) = R^3$.

Our results for the MEE for various prior distributions are shown in figures 1 to 5. In each of these figures we have also plotted the three model distributions obtained above. In figure 1 we have the MEE $\rho(R)$ for the choice $g(R) = 1$. It is seen that $\rho(R)$ vanishes at large R as expected, but remains finite at $R = 0$. In figures 2, 3 and 4 we have shown results for different choices of $g(R) = R^m$, $m = 1, 2, 3$, all of which vanish at $R = 0$—and so do the corresponding MEE, which also vanish as $R \to \infty$. We have also obtained the MEE of $\rho(R)$ for $g(R) = Re^{-R}$ shown in figure 5. The prior distribution $g(R) = Re^{-R}$ itself has a peak at $R = 1$. This fact is reflected in the corresponding $\rho(R)$ having two peaks. It is seen that the overall shape of the distribution is sensitive to the choice of a

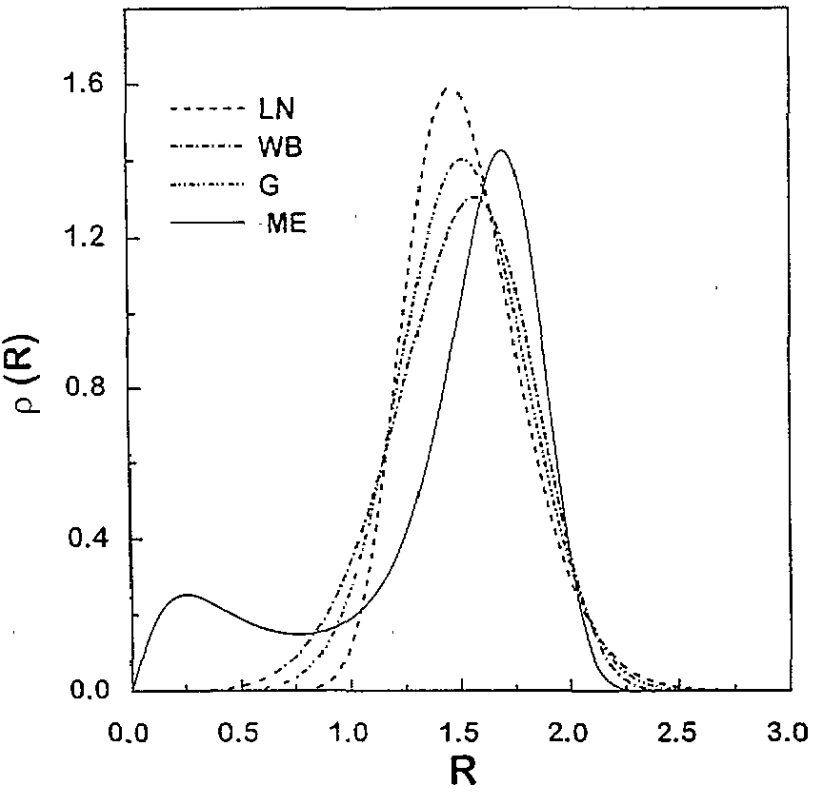

Figure 5. As figure 1, but with $g(R) = Re^{-R}$.

prior distribution; however, the peak in the distribution does not seem to be so sensitive.

We have computed the values of $\langle R \rangle$, $\langle R^2 \rangle$ and the value of the entropy S for the three model distributions and also for each of the MEEs. These results are summarized in table 1. For convenience, the MEE corresponding to $g(R) = R^m$, $m = 0, 1, 2, 3$, is denoted by ρ_m, and ρ_e denotes the MEE corresponding to $g(R) = Re^{-R}$. It is clear from table 1 that among the three model distributions the WB has the largest entropy. There is also an overall closeness between the WB distribution and the MEE corresponding to $g(R) = R^3$.

Table 1. Values of $\langle R \rangle$, $\langle R^2 \rangle$, the peak position and the entropy for the three model distributions and for the maximum-entropy estimates with different prior distributions.

Distribution function	$\langle R \rangle$	$\langle R^2 \rangle$	Peak position	Entropy S
LN	1.53	2.41	1.47	0.18
G	1.52	2.38	1.52	0.16
WB	1.50	2.36	1.57	0.23
ρ_0	1.23	1.89	1.66	0.52
ρ_1	1.44	2.23	1.64	0.39
ρ_2	1.48	2.31	1.61	0.30
ρ_3	1.5	2.34	1.59	0.25
ρ_e	1.41	2.24	1.70	0.42

Model distributions with adjustable parameters are usually intended to fit the given set of data and reflect a kind of bias of the experimentalist. They can, however, also serve as testing grounds for any novel prescription such as the maximum-entropy method. In this latter role one assumes that the exact real situation is described by, say, one of the LN, G or WB distributions with an assumed set of values for the adjustable parameters. This gives rise to an appropriate MSAS profile whose Porod and Guinier regime results lead to the moment ratios $a = 1.62$ and $b = 2.7$. With these moment ratios as input how does the MEE compare with the *actual* distribution? Figures 1 to 5 can be viewed from this perspective as well. One may also view the other two model distributions as model fits to the *actual* distribution. In this respect, the MEE generally seems to be reasonably good if the actual distribution happens to be the WB, but not so good if reality is represented either by the LN or by the G distribution.

For prior distributions of the form $g(R) = R^m$ we find that the peak in the maximum-entropy distribution becomes more pronounced and it shifts towards smaller values of R as m increases. A similar trend in the shape of the peak, but a shift in the opposite direction is seen in a simpler analogous problem. Here one is required to obtain the different MEEs for the probability distribution of a nonnegative random variate, which has the given mean value μ, using the different prior distributions listed above. This problem can be solved analytically. The probability distribution has a peak at $x = m\mu/(m+1)$. The peak becomes sharper and sharper and moves toward the value μ as m increases, and in the limit $m \to \infty$ the distribution assumes the shape of a δ-function centred at $x = \mu$

4. Conclusion

We have discussed the methodology for extracting the particle size distributions from MSAS profiles using the maximum-entropy method. Three model distributions have been used for comparison with the MEEs. We have noted that the maximum-entropy distributions strongly depend on the choice of prior distribution. The choice of prior distribution is an expression of bias. Among the three model distributions that we have examined the WB distribution is closer to the various MEEs and is closest to the ME results obtained using the prior distribution $g(R) \sim R^3$. In the absence of any concrete theoretical model for justifying the choice of any particular prior distribution, one must choose a uniform prior distribution that corresponds to the maximum entropy for the distribution function $\rho(R)$. It should be remembered that even with a uniform prior distribution the maximum-entropy estimate for $\rho(R)$ does have a peak at a finite value of R. This value of R, being not so sensitive to any particular choice of prior distribution, can be treated with confidence.

Finally, we have not considered possible error bars on the estimated moment ratios. It is possible to treat data with error bars within the framework of the maximum-entropy method; however, in the present paper the theme of interest was studying the sensitivity of MEEs to different prior distributions. With this in mind, we have excluded error bars from the present considerations.

References

[1] Mazumder S, Sequeira A, Roy S K and Biswas A R 1993 *J. Appl. Crystallogr.* **26** 357–62
[2] Kapur J N 1989 *Maximum Entropy Models in Science and Engineering* (New Delhi: Wiley Eastern)
[3] Morrison J D, Corcoran J D and Lewis K E 1992 *J. Appl. Crystallogr.* **25** 504–13
[4] Potton J A, Daniell G J and Rainford B D 1988 *J. Appl. Crystallogr.* **21** 663–8, 891–7

[5] Guerin D M A, Alvarez A G, Rebollo Neira L E, Plastino A and Bonetto R D 1986 *Acta. Crystallogr.* A **42** 30–5
[6] Rao S and Houska C R 1986 *Acta. Crystallogr.* A **42** 6–13
[7] Pederson J S 1993 *Phys. Rev.* B **47** 657–65
[8] Hansen S and Pederson J S 1991 *J. Appl. Crystallogr.* **24** 541–8
[9] Steenstrup S and Hansen S 1994 *J. Appl. Crystallogr.* **27** 574–80
[10] Mazumder S and Sequeira A 1992 *Pramana—J. Phys.* **38** 95–159